

New Magnetic Copper(II) Coordination Polymers with the Polynitrile Ligand $(\text{C}[\text{C}(\text{CN})_2]_3)^{2-}$ and N-Donor Co-ligands

Smaïl Triki,^{*,†} Franck Thétiot,[†] Fanny Vandavelde,[†] Jean Sala-Pala,[†] and Carlos J. Gómez-García[‡]

UMR CNRS 6521, Université de Bretagne Occidentale, BP 809, 29285 Brest Cedex, France, and Instituto de Ciencia Molecular, University of Valencia, Dr. Moliner 50, 46100 Burjasot, Spain

Received February 15, 2005

Reactions between CuCl_2 and K_2tcpd ($\text{tcpd}^{2-} = [\text{C}_{10}\text{N}_6]^{2-} = (\text{C}[\text{C}(\text{CN})_2]_3)^{2-}$) in the presence of neutral co-ligands (bpym = 2,2'-bipyrimidine, and tn = 1,3-diaminopropane) in aqueous solution yield the new compounds $[\text{Cu}_2(\text{bpym})(\text{tcpd})_2(\text{H}_2\text{O})_4] \cdot 2\text{H}_2\text{O}$ (**1**), $[\text{Cu}(\text{tn})(\text{tcpd})]$ (**2**), and $[\text{Cu}(\text{tn})_2(\text{tcpd})] \cdot \text{H}_2\text{O}$ (**3**), which are characterized by X-ray crystallography and magnetic measurements. Compound **1** displays a one-dimensional structure in which the bpym ligand, acting with a bis-chelating coordination mode, leads to $[\text{Cu}_2(\text{bpym})]^{4+}$ dinuclear units which are connected by two $\mu_2\text{-tcpd}^{2-}$ bridging ligands. Compound **2** consists of a three-dimensional structure generated by $[\text{Cu}(\text{tn})]^{2+}$ units connected by a $\mu_4\text{-tcpd}^{2-}$ ligand. The structure of **3** is made up of centrosymmetric planar $[\text{Cu}(\text{tn})]^{2+}$ units connected by a $\mu_2\text{-tcpd}^{2-}$ ligand leading to infinite zigzag chains. In compounds **1** and **3**, the bridging coordination mode of the tcpd^{2-} unit involves only two nitrogen atoms of one $\text{C}(\text{CN})_2$ wing, while in **2**, this ligand acts via four nitrogen atoms of two $\text{C}(\text{CN})_2$ wings. Despite this difference, the structural features of the tcpd^{2-} units in **1–3** are essentially similar. Magnetic measurements for compound **1** exhibit a maximum in the χ_m vs T plot (at ~ 150 K) which is characteristic of strong antiferromagnetic exchange interactions between the Cu(II) metal ions dominated by the magnetic exchange through the bis-chelating bpym. The fit of the magnetic data to a dimer model gives J and g values of -90.0 cm^{-1} and 2.12, respectively. For compounds **2** and **3** the thermal variations of the magnetic susceptibility show weak antiferromagnetic interactions between the Cu(II) metal ions that can be well reproduced with an antiferromagnetic regular $S = 1/2$ chain model that gives J values of $-0.07(2)$ and $-0.18(1) \text{ cm}^{-1}$ with g values of 2.12(1) and 2.13(1) for compounds **2** and **3**, respectively (the Hamiltonian is written in all the cases as $H = -JS_aS_b$).

Introduction

Polynitrile anions (Scheme 1)¹ have received, in the past few years, considerable interest in the field of coordination chemistry and molecular materials.² These organic anions are interesting for their high electronic delocalization and for their ability to act with various bridging coordination

modes since their cyano groups are juxtaposed in such a way that they cannot all coordinate to the same metal ion.^{3–9}

Thus, reactions of these organic anions with transition metal ions afford fascinating molecular extended structures of different dimensionalities and unusual magnetic properties;^{3–8} among them are the binary systems ML_n .^{3–9} For example, the tricoordinate dca^- ($\text{dca}^- = \text{dicyanamide} = \text{N}(\text{CN})_2^-$) and tcm^- ($\text{tcm}^- = \text{tricyanomethanide} = [\text{C}(\text{CN})_3]^-$) anions form rutile-like structures $\text{M}(\text{dca})_2$ and $\text{M}(\text{tcm})_2$ ($\text{M} = \text{Cr}(\text{II}), \text{Mn}(\text{II}), \text{Fe}(\text{II}), \text{Co}(\text{II}), \text{Ni}(\text{II}),$ and $\text{Cu}(\text{II})$),^{3,4} and the tetracoordinate tcpd^{2-} anion ($\text{tcpd}^{2-} = 2\text{-dicyanomethylene-1,1,3,3-tetracyanopropanediide} = [\text{C}_{10}\text{N}_6]^{2-} =$

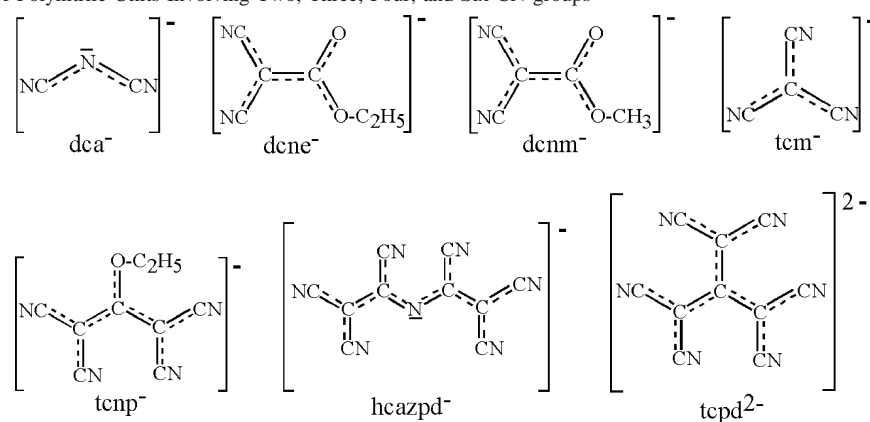
* To whom correspondence should be addressed. Fax: 33 298 017001. E-mail: smaïl.triki@univ-brest.fr.

[†] Université de Bretagne Occidentale (Brest).

[‡] Universidad de Valencia.

- (1) (a) Middleton, W. J.; Little, E. L.; Coffman, D. D.; Engelhardt, V. A. *J. Am. Chem. Soc.* **1958**, *80*, 2775. (b) Middleton, W. J.; Engelhardt, V. A. *J. Am. Chem. Soc.* **1958**, *80*, 2788. (c) Middleton, W. J.; Little, E. L.; Coffman, D. D.; Engelhardt, V. A. *J. Am. Chem. Soc.* **1958**, *80*, 2795. (d) Middleton, W. J.; Little, E. L.; Coffman, D. D.; Engelhardt, V. A. *J. Am. Chem. Soc.* **1958**, *80*, 2804. (e) Cairns, T. L.; McKusick, B. C. *Angew. Chem.* **1961**, *73*, 520. (f) Webster, O. W.; Mahler, W.; Benson, R. E. *J. Am. Chem. Soc.* **1962**, *84*, 3678. (g) Melby, L. R.; Harder, R. J.; Hertler, W. R.; Mahler, W.; Benson, R. E.; Mochel, W. E. *J. Am. Chem. Soc.* **1962**, *84*, 3374.

- (2) (a) Dunbar, K. R. *Angew. Chem., Int. Ed. Engl.* **1996**, *35*, 1659. (b) Kaim, W.; Moscherosch, M. *Coord. Chem. Rev.* **1994**, *129*, 157. (c) Manriquez, J. M.; Gordon, T. Y.; McLean, R. S.; Epstein, A. J.; Miller, J. S. *Science* **1991**, *252*, 1415. (d) Kato, R.; Kobayashi, H.; Kobayashi, A. *J. Am. Chem. Soc.* **1989**, *111*, 5224. (e) Miller, J. S.; Epstein, A. J.; Reiff, W. M. *Chem. Rev.* **1988**, *88*, 201.

Scheme 1. Examples of Polynitrile Units Involving Two, Three, Four, and Six CN groups

($\text{C}[\text{C}(\text{CN})_2]_3^{2-}$) (Scheme 1) forms an intriguing three-dimensional structure of formula $[\text{Cu}(\text{tcpd})(\text{H}_2\text{O})_2]$, generated by eclipsed chains which are laterally connected by equivalent eclipsed chains running orthogonally.⁸ Some of these 3D binary compounds show long-range magnetic ordering, hard magnetic behavior, or spin-canted antiferromagnetism.^{3,4}

To explore the influence of a second ligand on the network structures and on the electronic properties of these binary systems, various mixed-ligand compounds involving polynitrile and neutral bridging or chelating co-ligands have been reported.¹⁰ However, such mixed-ligand species have been limited to the simple polynitrile ligands such as dca, tcm,

and dcne ($\text{dcne}^- = 2,2\text{-dicyano-1-ethoxyethenolate} = [(\text{NC})_2\text{CC}(\text{O})\text{OEt}]^-$); mixed-ligand compounds involving sophisticated cyanocarbanions with more than three nitrile groups have not been reported yet. Herein, we report the syntheses, structural characterizations, and magnetic properties of three new compounds $[\text{Cu}_2(\text{bpym})(\text{tcpd})_2(\text{H}_2\text{O})_4] \cdot 2\text{H}_2\text{O}$ (**1**), $[\text{Cu}(\text{tn})(\text{tcpd})]$ (**2**), and $[\text{Cu}(\text{tn})_2(\text{tcpd})] \cdot \text{H}_2\text{O}$ (**3**) ($\text{tn} = 1,3\text{-diaminopropane} = \text{NH}_2\text{CH}_2\text{CH}_2\text{CH}_2\text{NH}_2$, and $\text{bpym} = 2,2'\text{-bipyrimidine} = \text{C}_8\text{H}_6\text{N}_4$) containing the tcpd^{2-} unit and involving either a bridging or a chelating ancillary ligand.

Experimental Section

General Methods. The reagents bpym (Lancaster), tn, and $\text{CuCl}_2 \cdot 2\text{H}_2\text{O}$ (Acros Organics) were used as received. K_2tcpd was prepared according to ref 1. All reactions were performed under aerobic conditions. Elemental analyses were obtained from the Service de microanalyses, CNRS, Gif sur Yvette, France. Infrared spectra were recorded in the range $4000\text{--}200\text{ cm}^{-1}$ as KBr pellets on a FT-IR NEXUS NICOLET Spectrometer. The magnetic studies were carried out on powder samples enclosed in medical caps. The magnetic susceptibility measurements were performed at 0.1 T, in the temperature range $2\text{--}300\text{ K}$ with a SQUID magnetometer MPMS-XL-5 from Quantum Design. The molar susceptibility was corrected from the sample holder and diamagnetic contributions of all atoms (Pascal's constants).

$[\text{Cu}_2(\text{bpym})(\text{tcpd})_2(\text{H}_2\text{O})_4] \cdot 2\text{H}_2\text{O}$ (1**).** An aqueous solution (2 mL) of 2,2'-bipyrimidine (50 mg, 0.316 mmol) was slowly added to a hot aqueous solution (2 mL) of $\text{CuCl}_2 \cdot 2\text{H}_2\text{O}$ (108 mg, 0.632 mmol). To the resulting solution was slowly added, with continuous stirring, an aqueous solution (5 mL) of potassium 2-dicyanomethylene-1,1,3,3-tetracyanopropanediide (179 mg, 0.632 mmol) leading to an immediate dark brown precipitate of **1** which was filtered and air-dried. Yield: 1.39 g (55%). Anal. Calcd. for $\text{C}_{28}\text{H}_{18}\text{-Cu}_2\text{N}_{16}\text{O}_6$: C, 41.96; H, 2.26; N, 27.96; Cu, 15.85%. Found: C, 42.10; H, 2.18; N, 28.08; Cu, 15.66%. IR data (ν/cm^{-1}): 3419br, 2244m, 2208s, 2192s, 1653w, 1588m, 1560w, 1507w, 1428s, 1413s, 1222w, 1032w, 741w, 687w, 537w, 482w. The crystalline powder was dissolved in hot water (40 mL) leading by slow evaporation to dark brown single crystals of **1** suitable for X-ray diffraction.

$[\text{Cu}(\text{tn})(\text{tcpd})]$ (2**) and $[\text{Cu}(\text{tn})_2(\text{tcpd})] \cdot \text{H}_2\text{O}$ (**3**).** 1,3-Diaminopropane (1.0 mL, 12.0 mmol) was added to a concentrated aqueous

- (3) (a) Pederson, M. R.; Liu, A. Y.; Baruah, T.; Kurmaev, E. Z.; Moewes, A.; Chiuzaibaian, S.; Neumann, M.; Kmety, C. R.; Stevenson, K. L.; Ederer, D. *Phys. Rev. C* **2002**, *66*, 014446/1–014446/8. (b) Van der Werff, P. M.; Batten, S. R.; Jensen, P.; Moubaraki, B.; Murray, K. S. *Inorg. Chem.* **2001**, *40*, 1718. (c) van der Werff, P. M.; Batten, S. R.; Jensen, P.; Moubaraki, B.; Murray, K. S.; Tan, E. H. K. *Polyhedron* **2001**, *20*, 1129. (d) Jensen, P.; Price, D. J.; Batten, S. R.; Moubaraki, B.; Murray, K. S. *Chem. Eur. J.* **2000**, *6*, 3186. (e) Batten, S. R.; Jensen, P.; Moubaraki, B.; Murray, K. S. *Chem. Commun.* **2000**, 2331. (f) Kmety, C. R.; Huang, Q.-Z.; Lynn, J. W.; Erwin, R. W.; Manson, J. L.; McCall, S.; Crow, J. E.; Stevenson, K. L.; Miller, J. S.; Epstein, A. J. *Phys. Rev. B* **2000**, *62*, 5576. (g) Batten, S. R.; Jensen, P.; Kepert, C. J.; Kurmoo, M.; Moubaraki, B.; Murray, K. S.; Price, D. J. *J. Chem. Soc., Dalton Trans.* **1999**, 2987. (h) Jensen, P.; Batten, S. R.; Fallon, G. D.; Moubaraki, B.; Murray, K. S.; Price, D. J. *Chem. Commun.* **1999**, 177. (i) Batten, S. R.; Jensen, P.; Moubaraki, B.; Murray, K. S.; Robson, R. *Chem. Commun.* **1998**, 439. (j) Kurmoo, M.; Kepert, C. J. *New J. Chem.* **1998**, *22*, 1515. (k) Manson, J. L.; Kmety, C. R.; Huang, Q. Z.; Lynn, J. W.; Bendele, G. M.; Pagola, S.; Stephens, P. W.; Liable-Sands, L. M.; Rheingold, A. L.; Epstein, A. J.; Miller, J. S. *Chem. Mater.* **1998**, *10*, 2552.
- (4) (a) Th  tiot, F.; Triki, S.; Sala Pala, J.; Golhen, S. *Inorg. Chim. Acta* **2003**, *350*, 314. (b) Feyerherm, R.; Loose, A.; Manson, J. L. *J. Phys.: Condens. Matter* **2003**, *15*, 663. (c) Manson, J. L.; Ressouche, E.; Miller, J. S. *Inorg. Chem.* **2000**, *39*, 1135. (d) Batten, S. R.; Hoskins, B. F.; Robson, R. *Chem. Eur. J.* **2000**, *6*, 156. (e) Batten, S. R.; Hoskins, B. F.; Moubaraki, B.; Murray, K. S.; Robson, R. *J. Chem. Soc., Dalton Trans.* **1999**, 2977. (f) Oshino, H.; Iida, K.; Kawamoto, T.; Mori, T. *Inorg. Chem.* **1999**, *38*, 4229. (g) Manson, J. L.; Campana, C.; Miller, J. S. *Chem. Commun.* **1998**, 251. (h) Batten, S. R.; Hoskins, B. F.; Robson, R. *New J. Chem.* **1998**, *22*, 173.
- (5) Kremer, C.; Meli  n, C.; Torres, J.; Juanic  , M. P.; Lamas, C.; Pezaroglo, H.; Manta, E.; Schumann, H.; Pickardt, J.; Girsigies, F.; Ventura, O. N.; Lloret, F. *Inorg. Chim. Acta* **2001**, *314*, 83.
- (6) Th  tiot, F.; Triki, S.; Sala Pala, J.; G  mez-Garc  a, C. J. *J. Chem. Soc., Dalton Trans.* **2002**, 1687.
- (7) Th  tiot, F.; Triki, S.; Sala Pala, J. *Polyhedron* **2003**, *22*, 1837.
- (8) (a) Triki, S.; Sala Pala, J.; Decoster, M.; Molini  , P.; Toupet, L. *Angew. Chem., Int. Ed. Engl.* **1999**, *38*, 113. (b) Triki, S.; Sala Pala, J.; Riou, A.; Molini  , P. *Synth. Met.* **1999**, *102*, 1472.
- (9) Decoster, M.; Guerchais, J. E.; Le Mest, Y.; Sala Pala, J.; Triki, S.; Toupet, L. *Polyhedron* **1996**, *15*, 195.

- (10) (a) Batten, S. R.; Murray, K. S. *Coord. Chem. Rev.* **2003**, *246*, 103, and references therein. (b) Th  tiot, F.; Triki, S.; Sala Pala, J.; Gal  n-Mascar  s, J. R.; Mart  nez-Agudo, J. M.; Dunbar, K. R. *Eur. J. Inorg. Chem.* **2004**, 3783.

solution (10 mL) of $\text{CuCl}_2 \cdot 2\text{H}_2\text{O}$ (2.04 g, 12.0 mmol) with continuous stirring, leading to the immediate precipitation of a green powder. After addition of an aqueous solution (10 mL) of sodium hydroxide (0.48 g, 12.0 mmol), the resulting dark blue solution was warmed (about 60 °C for about 5 min) and then filtered in order to eliminate the precipitate which remained. An aqueous solution (1 mL) of $\text{CuCl}_2 \cdot 2\text{H}_2\text{O}$ (0.68 g, 4.0 mmol) was then added, and the resulting solution was treated with an aqueous solution (30 mL) of potassium 2-dicyanomethylene-1,1,3,3-tetracyanopropane-diide (3.39 g, 12.0 mmol); this resulted in the immediate precipitation of a green powder which was dissolved, after filtration, in hot water. The final solution yielded by slow evaporation green crystals of **2** and mauve crystals of **3** which were separated manually. Anal. Calcd for $\text{C}_{13}\text{H}_{10}\text{CuN}_8$ (**2**): C, 45.68; H, 2.95; N, 32.78; Cu, 18.59%. Found: C, 45.81; H, 3.06; N, 32.38; Cu, 18.28%. IR data (ν/cm^{-1}): 3436m, 3308m, 3242m, 3141w, 2230s, 2191s, 2175s, 1586w, 1410s, 1165m, 1014m, 926w, 880w, 678m, 636w, 536w, 495w, 477w. Anal. Calcd for $\text{C}_{16}\text{H}_{22}\text{CuN}_{10}\text{O}$ (**3**): C, 44.28; H, 5.11; N, 32.28; Cu, 14.64%. Found: C, 43.98; H, 5.01; N, 32.51; Cu, 14.87%. IR data (ν/cm^{-1}): 3446m, 3314m, 3284m, 3250w, 2184s, 2165s, 1605m, 1590m, 1421s, 1167m, 1020m, 911m, 802w, 669m, 536m, 481m.

As mentioned above, equimolar reaction between $\text{CuCl}_2 \cdot 2\text{H}_2\text{O}$ and 1,3-diaminopropane, in the presence of sodium hydroxide, leads to the formation of a mixture of $[\text{Cu}(\text{tn})(\text{H}_2\text{O})_n]^{2+}$ and $[\text{Cu}(\text{tn})_2(\text{H}_2\text{O})_m]^{2+}$ entities since a mixture of compounds **2** and **3** was obtained. However, slight modifications of the synthetic procedure allowed the formation of **3** as a single compound: a large excess of 1,3-diaminopropane (3.6 mL, 43.2 mmol) was added to a concentrated aqueous solution of $\text{CuCl}_2 \cdot 2\text{H}_2\text{O}$ (2.04 g, 12.0 mmol) with continuous stirring, leading to the immediate formation of a blue solution to which was slowly added, with continuous stirring, an aqueous solution (10 mL) of K_2tcpd (3.39 g, 12.0 mmol). This resulted in the immediate precipitation of a mauve powder which was dissolved, after filtration, in hot water. Slow evaporation of the resulting solution gave mauve crystals of **3**; they were filtered and air-dried. Yield: 2.71 g (52%).

X-ray Structure Determinations. Data were collected at $T = 288$ K on a Xcalibur 2 Diffractometer (Oxford Diffraction) using a graphite monochromated Mo $\text{K}\alpha$ radiation ($\lambda = 0.71073$ Å). The structures were solved by direct methods and successive Fourier difference syntheses, and were refined on F^2 by weighted anisotropic full-matrix least-squares methods.¹¹ For **1**, all hydrogen atoms were located by difference Fourier maps; the hydrogen atoms of the bpym ligand were refined isotropically, while those of the three water molecules were not refined. For **2** and **3**, the hydrogen atoms were calculated [$d(\text{C}-\text{H}) = 0.95$ Å], except for the two hydrogen atoms of the water molecule of **3** which were not included; the thermal parameters were taken as $U_{\text{iso}} = 1.3 U_{\text{equ}}(\text{C})$ and therefore included as isotropic fixed contributors to F_c . Scattering factors and corrections for anomalous dispersion were taken from the *International Tables for X-ray Crystallography*.¹² The thermal ellipsoid drawings were made with the ORTEP program.¹³ All calculations were performed on an Alphastation 255 4/233 computer. Pertinent crystal data and selected bond distances and bond angles are listed in Tables 1–3. Complete crystallographic details are included in the Supporting Information.

Table 1. Crystallographic Data and Structural Refinement Parameters for Compounds $[\text{Cu}_2(\text{bpym})(\text{tcpd})_2(\text{H}_2\text{O})_4] \cdot 2\text{H}_2\text{O}$ (**1**), $[\text{Cu}(\text{tn})(\text{tcpd})]$ (**2**), and $[\text{Cu}(\text{tn})_2(\text{tcpd})] \cdot \text{H}_2\text{O}$ (**3**)

	1	2	3
formula	$\text{C}_{28}\text{H}_{18}\text{N}_{16}\text{O}_6\text{Cu}_2^a$	$\text{C}_{13}\text{H}_{10}\text{N}_8\text{Cu}$	$\text{C}_{16}\text{H}_{22}\text{N}_{10}\text{OCu}$
Fw	801.64	341.82	433.96
cryst. system	triclinic	monoclinic	triclinic
space group	P-1	$P2_1/n$	P-1
a (Å)	7.7495(4)	7.3655(9)	9.891(2)
b (Å)	9.8432(6)	13.955(2)	9.955(2)
c (Å)	10.9787(8)	14.337(2)	11.608(2)
α (°)	97.6(2)	90	73.11(2)
β (°)	101.2(2)	94.72(1)	66.83(2)
γ (°)	90.076(5)	90	77.32(2)
V (Å ³)	814.1(9)	1468.7(5)	998.2(3)
ρ_{calcd} , (g cm ⁻³)	1.64	1.55	1.44
Z	1	4	2
μ (cm ⁻¹)	13.76	14.97	11.23
$R(F_o)^b$	0.045	0.071	0.029
$R_w(F_o)^c$	0.050	0.076	0.030
GOF ^d	1.006	1.225	1.102

^a The asymmetric unit contains 0.5 of the chemical formula. ^b $R = \sum |F_o| - |F_c| / \sum |F_o|$. ^c $R_w = [\sum w(|F_o| - |F_c|)^2 / \sum w(F_o)^2]^{1/2}$. ^d $\text{GOF} = [(\sum w|F_o| - |F_c|)^2 / (N_{\text{obs}} - N_{\text{var}})]^{1/2}$.

Table 2. Important Bond Lengths (Å) and Angles (deg) for Compounds **1–3**

	1	2	3		
Cu–N1	1.955(3)	Cu–N1	1.996(8)	Cu1–N1	2.551(5)
Cu–N2	1.980(4)	Cu–N2	2.346(9)	Cu1–N7	2.038(5)
Cu–O1	2.371(3)	Cu–N3	2.71(1)	Cu1–N8	2.020(4)
Cu–O2	2.344(3)	Cu–N4	1.991(8)	Cu2–N2	2.578(4)
Cu–N7	2.063(4)	Cu–N7	2.015(8)	Cu2–N9	2.022(5)
Cu–N8	2.043(3)	Cu–N8	1.996(8)	Cu2–N10	2.002(3)
N1–Cu–N2	91.0(1)	N1–Cu–N2	94.4(3)	N1–Cu1–N7	87.0(2)
N1–Cu–N7	93.3(1)	N1–Cu–N3	95.5(3)	N1–Cu1–N8	90.9(2)
N1–Cu–N8	173.4(2)	N1–Cu–N4	90.1(3)	N7–Cu1–N8	89.6(2)
N1–Cu–O1	94.0(1)	N1–Cu–N7	87.1(3)	N2–Cu2–N9	90.2(2)
N1–Cu–O2	90.3(1)	N1–Cu–N8	175.6(3)	N2–Cu2–N10	91.2(1)
N2–Cu–N7	175.1(1)	N2–Cu–N3	169.8(3)	N9–Cu2–N10	89.5(2)
N2–Cu–N8	95.0(1)	N2–Cu–N4	95.7(3)		
N2–Cu–O1	87.1(1)	N2–Cu–N7	95.5(3)		
N2–Cu–O2	88.1(1)	N2–Cu–N8	89.7(3)		
N7–Cu–N8	80.8(1)	N3–Cu–N4	86.7(3)		
N7–Cu–O1	90.3(1)	N3–Cu–N7	82.6(3)		
N7–Cu–O2	94.2(1)	N3–Cu–N8	80.4(3)		
N8–Cu–O1	89.0(1)	N4–Cu–N7	168.7(3)		
N8–Cu–O2	87.2(1)	N4–Cu–N8	88.1(3)		
O1–Cu–O2	173.6(1)	N7–Cu–N8	93.9(3)		

Results and Discussion

Syntheses and General Characterization. Reaction in aqueous solution of copper(II) chloride with 2,2'-bipyrimidine (bpym) and potassium 2-dicyanomethylene-1,1,3,3-tetracyanopropane-diide K_2tcpd gives, after further workup, the new compound $[\text{Cu}_2(\text{bpym})(\text{tcpd})_2(\text{H}_2\text{O})_4] \cdot 2\text{H}_2\text{O}$ (**1**) as dark brown crystals. A similar reaction performed in the presence of sodium hydroxide with 1,3-diaminopropane (tn) instead of bpym (molar ratio $\text{tn}/\text{Cu} = 1$) affords a mixture of $[\text{Cu}(\text{tn})(\text{tcpd})]$ (**2**) and $[\text{Cu}(\text{tn})_2(\text{tcpd})] \cdot \text{H}_2\text{O}$ (**3**) as green and mauve crystals, respectively. The use of a large excess of tn (molar ratio $\text{tn}/\text{Cu} > 3$) gives exclusively $[\text{Cu}(\text{tn})_2(\text{tcpd})] \cdot \text{H}_2\text{O}$ (**3**) as mauve crystals. Attempts to obtain complex **2** as a single compound failed since all the synthetic procedures used afford mixtures of the two compounds.

IR spectra of compounds **1–3** present the usual absorption bands of the tcpd^{2-} unit and specifically several bands, in

(11) Fair, C. K. *MolEN, An Interactive Intelligent System for Crystal Structure Analysis*, User Manual; Enraf-Nonius: Delft, The Netherlands, 1985.

(12) *International Tables for X-ray Crystallography*; Kynoch Press: Birmingham, U.K., 1975; Vol. 4.

(13) Johnson, C. K. *ORTEP*, Rep. ONL-3794, Delft, The Netherlands, 1985.

Table 3. Bond Lengths (Å) and Angles (deg) for the tcpd^{2-} Ligands in Compounds 1–3

	1	2	3
N1–C1	1.155(5)	1.14(1)	1.142(6)
N2–C2	1.146(6)	1.13(1)	1.150(6)
N3–C3	1.149(9)	1.13(1)	1.133(8)
N4–C4	1.147(6)	1.14(1)	1.138(6)
N5–C5	1.158(8)	1.14(2)	1.132(7)
N6–C6	1.154(7)	1.17(1)	1.143(8)
C1–C8	1.390(5)	1.41(1)	1.413(6)
C2–C8	1.396(6)	1.41(1)	1.424(6)
C3–C9	1.421(8)	1.40(1)	1.407(8)
C4–C9	1.416(6)	1.41(1)	1.411(6)
C5–C10	1.441(8)	1.42(2)	1.412(7)
C6–C10	1.447(7)	1.39(2)	1.406(9)
C7–C8	1.449(6)	1.42(1)	1.404(6)
C7–C9	1.410(6)	1.40(1)	1.424(7)
C7–C10	1.382(7)	1.44(1)	1.420(7)
N1–C1–C8	178.5(5)	178(1)	177.6(7)
N2–C2–C8	177.5(4)	176(1)	178.6(7)
N3–C3–C9	179.0(6)	178(1)	178.4(6)
N4–C4–C9	176.8(7)	176(1)	176.0(5)
N5–C5–C10	176.2(6)	175(1)	178.8(5)
N6–C6–C10	178.7(6)	175(1)	177.2(5)
C8–C7–C9	119.2(4)	122.2(8)	120.1(4)
C8–C7–C10	118.1(4)	119.6(9)	119.9(5)
C9–C7–C10	122.6(4)	118.1(9)	120.0(4)
C1–C8–C2	115.8(4)	116.1(8)	115.3(4)
C1–C8–C7	121.5(4)	121.9(8)	122.3(4)
C2–C8–C7	122.7(3)	121.9(9)	122.4(4)
C3–C9–C4	113.0(4)	116.3(9)	115.5(5)
C3–C9–C7	123.4(4)	121.4(9)	121.6(4)
C4–C9–C7	123.6(5)	122.2(8)	122.9(5)
C5–C10–C6	114.9(5)	116(1)	115.8(4)
C5–C10–C7	123.0(4)	121(1)	122.3(5)
C6–C10–C7	121.1(5)	122(1)	122.0(5)

the 2250–2160 cm^{-1} range, assigned to ν_{CN} . Compared to the corresponding potassium salt (K_2tcpd) containing the non coordinated tcpd^{2-} moiety (2191 and 2121 cm^{-1}), the ν_{CN} values observed in these spectra (2244, 2208, and 2192 for **1**; 2230, 2191, and 2175 for **2**; 2184 and 2165 cm^{-1} for **3**) are indicative of the presence of coordinated and noncoordinated nitrile groups in the three compounds. Concerning the bpym ligand which can act either as a terminal chelating or a bis(chelating) ligand toward transition metal ions, previous studies show that IR spectroscopy can be used as a diagnostic tool for identifying the coordination mode.^{14,15} The terminal chelating mode is typically characterized by two intense, sharp peaks of nearly equal intensities at approximately 1580 and 1560 cm^{-1} (ring stretching modes of

(14) De Munno, G.; Julve, M. *NATO ASI Ser. Ser. C* **1996**, 474, 139, and references therein.

(15) For Cu–bpym complexes, see for example (a) Rorríguez-Martin, Y.; Sanchiz, J.; Ruiz-Pérez, C.; Lloret, F.; Julve, M. *Inorg. Chim. Acta* **2001**, 326, 20. (b) De Munno, G.; Poerio, T.; Julve, M.; Lloret, F.; Faus, J.; Caneschi, A. *J. Chem. Soc., Dalton Trans.* **1998**, 1679. (c) De Munno, G.; Julve, M.; Lloret, F.; Cano, J.; Caneschi, A. *Inorg. Chem.* **1995**, 34, 2048. (d) De Munno, G.; Julve, M.; Lloret, F.; Faus, J.; Verdager, M.; Caneschi, A. *Inorg. Chem.* **1995**, 34, 157. (e) Castro, I.; Sletten, J.; Glaerum, L. K.; Cano, J.; Lloret, F.; Faus, J.; Julve, M. *J. Chem. Soc., Dalton Trans.* **1995**, 3207. (f) Castro, I.; Sletten, J.; Glaerum, L. K.; Lloret, F.; Faus, J.; Julve, M. *J. Chem. Soc., Dalton Trans.* **1994**, 2777. (g) De Munno, G.; Real, J. A.; Julve, M.; Munoz, M. C. *Inorg. Chim. Acta* **1993**, 211, 227. (h) De Munno, G.; Julve, M.; Nicolo, F.; Lloret, F.; Faus, J.; Ruiz, R.; Sinn, E. *Angew. Chem., Int. Ed. Engl.* **1993**, 32, 613. (i) De Munno, G.; Julve, M.; Lloret, F.; Faus, J.; Ruiz, R.; Sinn, E. *Angew. Chem., Int. Ed. Engl.* **1993**, 32, 1046. (j) De Munno, G.; Julve, M.; Verdager, M.; Bruno, G. *Inorg. Chem.* **1993**, 32, 2215. (k) Julve, M.; Verdager, M.; De Munno, G.; Real, J. A.; Bruno, G. *Inorg. Chem.* **1993**, 32, 795.

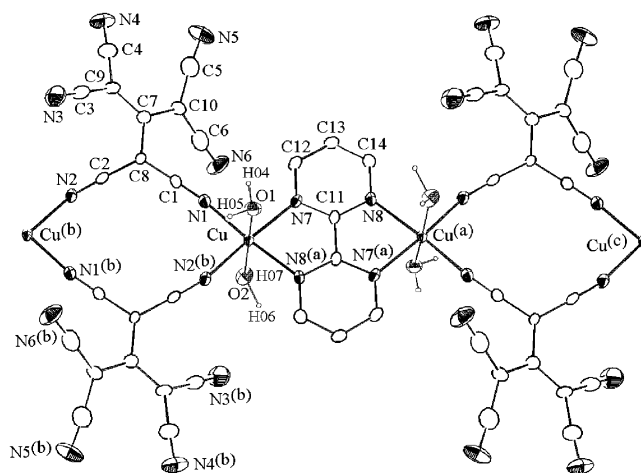


Figure 1. ORTEP view of compound **1** showing the atom labeling scheme, the Cu(II) environment, and the 1D structure. Codes of the equivalent positions: (a) $-x, -y, -z$, (b) $1-x, 1-y, -z$, and (c) $-1+x, -1+y, z$.

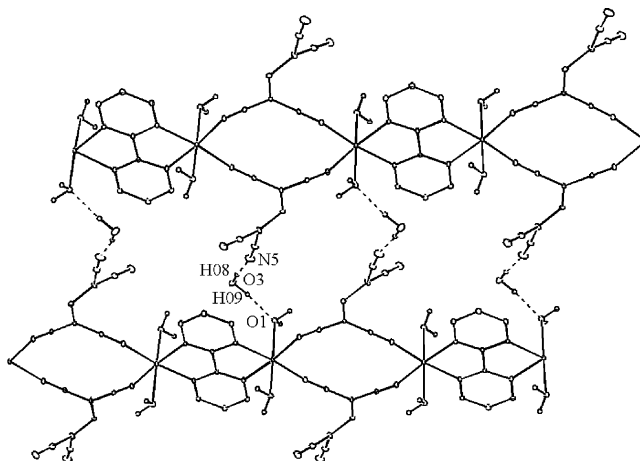


Figure 2. ORTEP view of compound **1** showing the 2D structure generated through hydrogen bonding between adjacent chains (dashed lines). One of the two uncoordinated wings of the tcpd^{2-} ligand is omitted for clarity.

bpym); the presence of the bis-chelating coordination mode is indicated either by an asymmetric doublet or a single strong broad feature around 1580 cm^{-1} .^{14,15} The asymmetric doublet observed in the IR spectrum (1588 and 1560 cm^{-1}) points to the presence of the bis-chelating coordination mode of the bpym in compound **1**.

Crystal Structures of $[\text{Cu}_2(\text{bpym})(\text{tcpd})_2(\text{H}_2\text{O})_4] \cdot 2\text{H}_2\text{O}$ (1**), $[\text{Cu}(\text{tn})(\text{tcpd})]$ (**2**), and $[\text{Cu}(\text{tn})_2(\text{tcpd})] \cdot \text{H}_2\text{O}$ (**3**).** ORTEP plots of compounds **1**, **2**, and **3** are shown in Figures 1–5. Pertinent crystal data, interatomic distances, and angles are listed in Tables 1–3, respectively.

For compound **1**, the asymmetric unit consists of one copper(II) ion, one bpym molecule on a special position (0,0,0), one tcpd^{2-} anion, and three water molecules. Each metal ion is linked to four nitrogen atoms (two from the bis-chelating bpym, two from two polynitrile ligands) and to two water molecules in the trans configuration (Figure 1).

The CuN_4O_2 octahedron can be viewed as a planar array, within ± 0.001 Å, of four short Cu–N bonds in the range 1.955–2.063 Å with two trans long Cu–O ones (2.371(3) and 2.344(3) Å). As shown in Figure 1, the tcpd^{2-} anion acts as a bridging ligand via two nitrogen atoms of one of

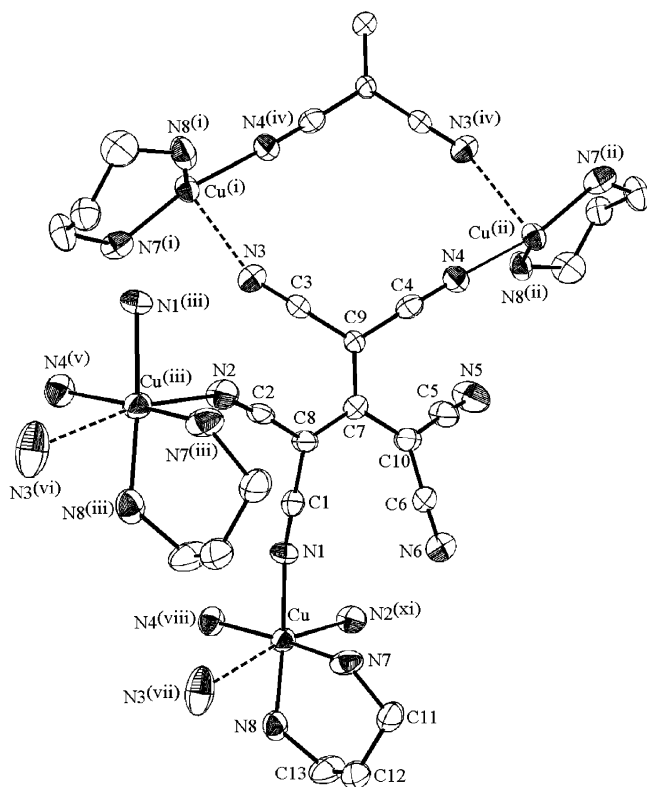


Figure 3. ORTEP view showing the atomic labeling scheme, the asymmetric unit, the μ_4 -tcpd $^{2-}$ ligand, and the metal ion environment in **2**. Cu \cdots Cu distances (\AA): Cu $^{(i)}\cdots$ Cu $^{(iii)}$ 6.981(2), Cu \cdots Cu $^{(iii)}$ 7.366(2), Cu $^{(i)}\cdots$ Cu $^{(ii)}$ 7.630(2), Cu $^{(ii)}\cdots$ Cu $^{(iii)}$ 9.924(2), Cu \cdots Cu $^{(i)}$ 10.065(2), and Cu \cdots Cu $^{(ii)}$ 10.352(2). Codes of equivalent positions: (i) $-1/2-x, 1/2+y, 1/2-z$; (ii) $-1/2+x, 1/2-y, 1/2+z$; (iii) $-1+x, y, z$; (iv) $-1-x, 1-y, 1-z$; (v) $-1/2+x, 1/2-y, -1/2+z$; (vi) $-3/2-x, -1/2+y, 1/2-z$; (vii) $-1/2-x, -1/2+y, 1/2-z$; (viii) $1/2+x, 1/2-y, -1/2+z$; (ix) $1+x, y, z$.

its three C(CN) $_2$ wings. This leads to almost planar 12-membered (Cu(NCCCN) $_2$ Cu) dimetallacycles; these dimetallacycles are connected to each other by the bis-chelating bpyim to give a 1D chain running along the [110] direction. The Cu \cdots Cu distance through the bis-chelating ligand (5.5047(8) \AA) is in the usual range for this bridge (5.38–5.55 \AA); 10,15 as expected, the Cu \cdots Cu distance through the bridging polynitrile ligand (7.0203(8) \AA) is similar to that observed in the binary system Cu–tcpd (7.026 \AA). 8 An examination of the intermolecular distances between adjacent chains reveals hydrogen bonds involving coordinated and noncoordinated water molecules (H04–O1–H05 and H08–O3–H09, respectively) and a noncoordinated nitrile group (N5) of the tcpd $^{2-}$ ligand (O1 \cdots H09 1.86 \AA , H09–O3 0.90 \AA , N5 \cdots H08 1.81 \AA , H08–O3 1.03 \AA , O1 \cdots H09–O3 172.7 $^\circ$, N5 \cdots H08–O3 169.0 $^\circ$), giving rise to an overall 2D structure as highlighted in Figure 2.

For compound **2**, the asymmetric unit consists of one [Cu(tn)] $^{2+}$ unit and one tcpd $^{2-}$ anion, both located on general positions. Each Cu atom presents a CuN $_4$ N $_2$ distorted octahedral coordination with four nitrogen atoms arising from four polynitrile ligands and two nitrogen atoms from the chelating tn ligand (Figure 3). The Cu(II) coordination octahedron is much more severely distorted here than in compound **1**. While the CuN1N4N7N8 is almost planar within ± 0.2 \AA and presents almost equivalent Cu–N bond

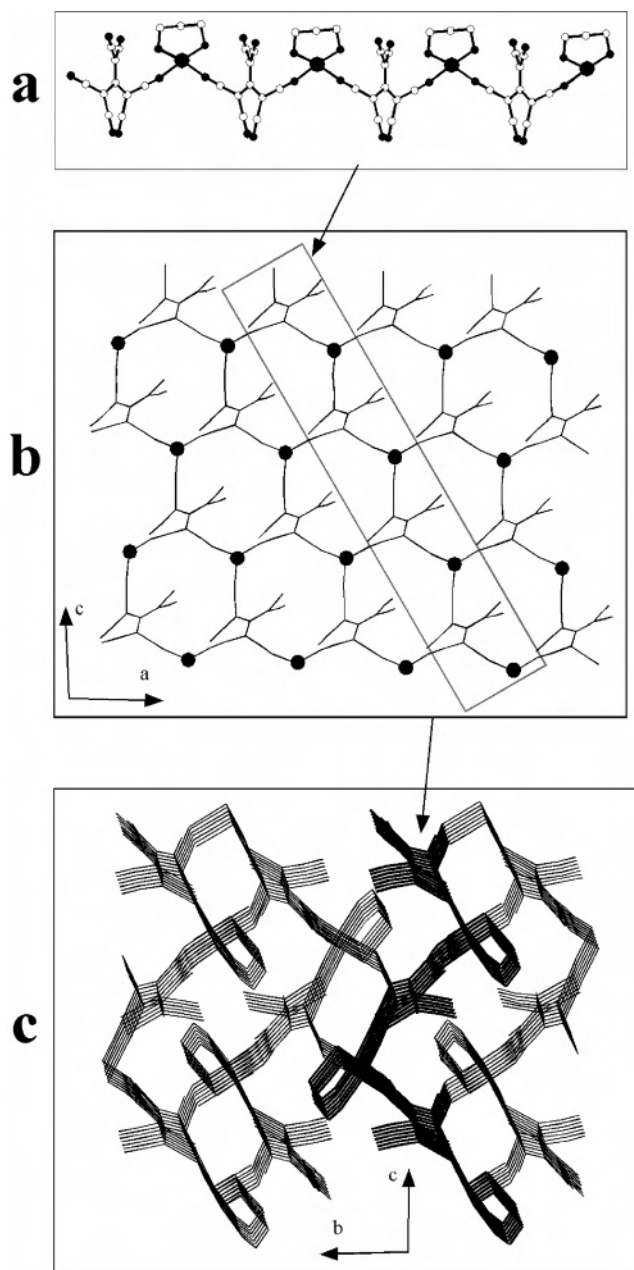


Figure 4. Three-dimensional molecular arrangement of **2**: (a) The 1D motif generated when the tcpd ligand is viewed as a μ_2 -bridging ligand (Cu–N1 and Cu–N4 bonds < 2.0 \AA). (b) The 2D motif observed when the tcpd ligand is viewed as a μ_3 -bridging ligand (Cu–N1, Cu–N4, and Cu–N2 bonds < 2.35 \AA), the tn ligands are omitted for clarity. (c) The 3D structure of **2** generated with the μ_4 -bridging ligand.

lengths [1.991(8) and 1.996(8) \AA from the polynitrile ligand; 1.996(8) and 2.015(8) \AA from the tn ligand], the two *trans*-CuN2 and CuN3 bonds are much longer [2.346(9) and 2.71(1) \AA , respectively].

The coordination mode of the tcpd $^{2-}$ anion is very different from that observed for compound **1** since, here, this ligand acts with a μ_4 -bridging mode via four nitrogen atoms of two different C(CN) $_2$ wings (Figure 3) leading to the 3D structure depicted in Figure 4c. The shortest Cu \cdots Cu distance through the tcpd $^{2-}$ ligand corresponds to that observed between two different C(CN) $_2$ wings (Cu $^{(i)}\cdots$ Cu $^{(iii)}$ 6.981(2) \AA); whereas the Cu \cdots Cu distances observed through the same C(CN) $_2$

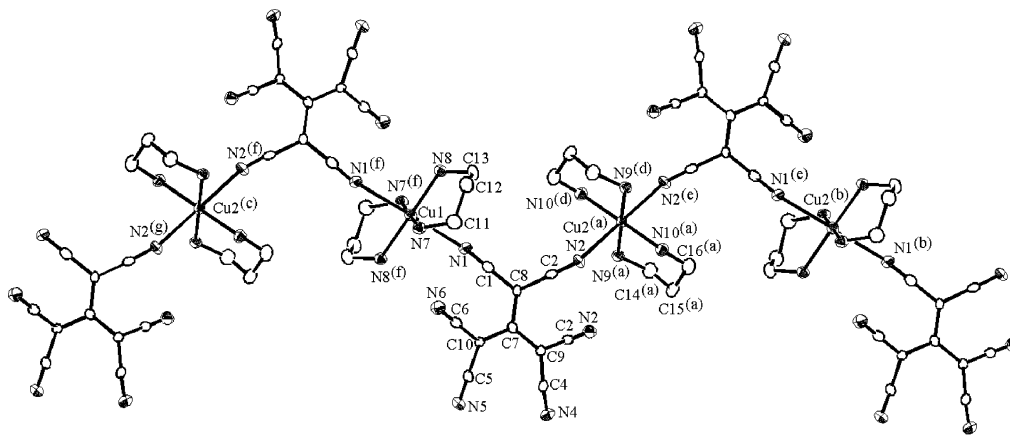


Figure 5. ORTEP view showing the atomic labeling scheme, the asymmetric unit, the μ_2 -tcpd $^{2-}$ ligand, and the metal ion environment in **3**. Codes of equivalent positions: (a) $x, 1+y, 1+z$; (b) $-1+x, 1+y, 1+z$; (c) $1+x, y, z$; (d) $-x, -y, 2-z$; (e) $-x, 1-y, 3-z$; (f) $1-x, -y, 2-z$; (g) $1+x, -1+y, -1+z$.

wing are slightly longer (Cu \cdots Cu $^{(iii)}$ 7.366(2) and Cu $^{(i)}\cdots$ Cu $^{(ii)}$ 7.630(2) Å).

It is worthy to note that the tcpd $^{2-}$ unit can also be described as an essentially μ_3 -ligand (Figure 4b) and therefore the Cu coordination polyhedron as a moderately elongated square base pyramid since the Cu–N3 distance is rather long. Thus, the simplest way to describe the complicated 3D molecular arrangement is to consider the 2D elemental unit generated by a μ_3 -bridging tcpd $^{2-}$ ligand as shown in Figure 4a,b. These layers are connected to each other through the long N3 \cdots Cu bridges to lead to the 3D structure of **2** (Figure 4c).

For compound **3**, the structure is built from two crystallographically independent [Cu(tn)] $^{2+}$ units (Cu1 and Cu2), both located on inversion centers, and one tcpd $^{2-}$ anion on a general position. The two [Cu(tn) $_2$] $^{2+}$ units present essentially similar structural features with the Cu atom in a CuN $_4$ N $_2$ distorted octahedral coordination with four nitrogen atoms arising from two tn chelating ligands (Cu–N from 2.002(3) to 2.038(5) Å) and two nitrogen atoms from the tcpd $^{2-}$ ligand (Cu–N: 2.551(5) and 2.578(4) Å) (Figure 5). As in compound **1**, the tcpd $^{2-}$ ligand acts with a μ_2 -bridging mode via two nitrogen atoms of one C(CN) $_2$ wing, but it is only weakly bound to the copper atom (shortest Cu–N: 2.551 Å in **3**, 1.955 Å in **1**, and 1.991 Å in **2**). This leads to a 1D chain running along the [1, –1, –1] direction (Figure 5). The intrachain Cu \cdots Cu distance through the tcpd $^{2-}$ ligand (Cu1 \cdots Cu2 8.1433(1) Å) is longer than the interchain Cu1 \cdots Cu2 one (7.3724(1) Å).

Structure of the tcpd $^{2-}$ Ligand. As clearly described above, despite its six potentially bridging nitrile groups, the tcpd $^{2-}$ ligand shows only a μ_4 - (or at least μ_3) bridging coordination mode in compound **2** and a μ_2 -bridging coordination mode in compounds **1** and **3**, with a stronger metal–ligand interaction in **1** than in **3** as indicated by shorter CuN bond lengths. Despite these differences, this organic ligand roughly presents similar features in compounds **1–3** as shown by the crystallographic parameters depicted in Table 3. The central fragment of each tcpd $^{2-}$ ligand is essentially planar (maximum deviation of 0.01 Å) and is built on carbon atoms (C7, C8, C9, and C10) showing sp 2 hybridization. Careful examination of the tilt angles between

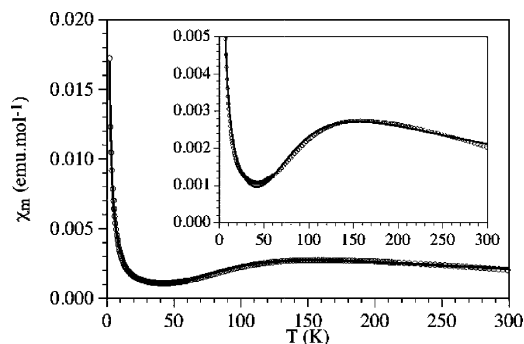


Figure 6. Thermal variation of the magnetic susceptibility in the form of χ_m versus T for compound **1**. Inset: a close view of the maximum and the minimum in the plot. The solid line represents the best fit to the model (see text).

the mean central plane and the three C(CN) $_2$ wing planes reveals that the structure and the symmetry of the ligand are affected by the coordination modes. Thus, while in compounds **2** and **3** the three tilt angles out of the central plane deviate moderately from the average value (23.2, 26.3, and 27.2° in **2**, 24.4, 24.5, and 25.2° in **3**), in compound **1** this deviation is much more pronounced (14.9, 22.5, and 31.8°). Note that the largest and smallest values correspond to the coordinated N1N2 and to the hydrogen-bonded N5N6 wings, respectively. The propeller-shaped geometry, previously reported for the tcpd $^{2-}$ unit, 8,16 decreases the CN \cdots NC steric interactions between the nitrile groups of adjacent C(CN) $_2$ wings, but does not preclude an intense electronic delocalization all over the ligand (Table 3). This high electronic delocalization is similar to those previously reported for this ligand 8,16 and for less sophisticated polynitrile ligands. 6,7

Magnetic Properties. The magnetic properties for compounds **1–3** are displayed in Figures 6 and 7 as the thermal variation of the molar magnetic susceptibility per formula unit (χ_m) for **1** and as $\chi_m T$ versus T for **2** and **3**. In compound **1** the thermal variation of χ_m presents a broad maximum at approximately 150 K, which is consistent with the presence of strong antiferromagnetic interactions between the metal ions. The increase observed below 50 K is attributed to the presence of paramagnetic impurities (Figure 6).

(16) Bekoe, D.; Gantzel, P. K.; Trueblood, K. N. *Acta Crystallogr.* **1967**, *22*, 657.

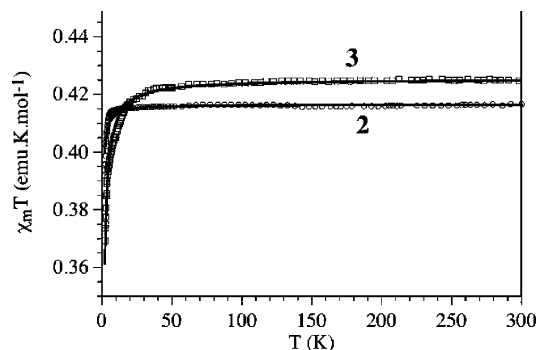


Figure 7. Thermal variation of the product of the molar magnetic susceptibility times the temperature for compounds **2** and **3**. Solid lines are the best fits to the model (see text).

The magnetic data previously reported for the 3D compound [Cu(tcpd)(H₂O)₂] involving bridges similar to those described here for compound **1**⁸ and examination of several related compounds involving the Cu–bpym–Cu bridges¹⁵ suggest that the magnetic interactions through the tcpd²⁻ bridges are much weaker than those observed through the bpym bridges ($|J_{\text{tcpd}}| < 0.5 \text{ cm}^{-1}$ and $|J_{\text{bpym}}| > 90 \text{ cm}^{-1}$ for Cu(II)). Accordingly, we have fitted the magnetic data with the isotropic $S = 1/2$ dimer model of Bleaney and Bowers,¹⁷ taking only into account the interactions through the bpym ligand (the Hamiltonian is written as $H = -2JS_aS_b$) and adding a term for the paramagnetic contribution. A very satisfactory fit over the whole temperature range (2–300 K) is obtained with the following set of parameters: $J = -90 \text{ cm}^{-1}$, $g = 2.12$, and 4% of monomeric paramagnetic impurity (solid line in Figure 6). The J value is similar to those found in other Cu–bpym–Cu bridges.¹⁵ Note that a more sophisticated model including the magnetic interactions through the tcpd²⁻ bridges (as J') can also be considered. Nevertheless, the very high $|J|/|J'|$ ratio precludes any conclusive estimation of J' since the final plot is almost independent of the changes in the J' value or in its sign.

For compound **2**, the thermal variation of the product of the molar magnetic susceptibility times the temperature ($\chi_m T$) shows a constant value of about $0.41 \text{ emu K mol}^{-1}$ from room temperature down to about 10 K (Figure 7). Below this temperature the $\chi_m T$ product shows a weak decrease, indicative of the presence of very weak antiferromagnetic interactions, to reach a value of $0.39 \text{ emu K mol}^{-1}$ at 2 K (Figure 7).

According to the structural results obtained for this compound, the axial interaction through the two longest Cu–N distances (Cu–N3 2.71(1) and Cu–N2 2.346(9) Å) can be neglected to simplify its 3D arrangement. In this case, the structure of **2** can be viewed as a 1D chain (see “...Cu–N1...N4–Cu...” chain in Figures 3 and 4a), and then, the weak antiferromagnetic behavior could be explained by intrachain interaction between neighboring copper ions. Thus, a further analysis was restricted to the 1D model; the experimental data were fitted using the empirical expression proposed by Hatfield^{18,19} for antiferromagnetic 1D isotropic

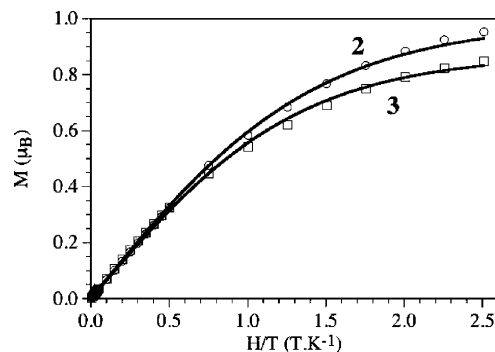


Figure 8. Isothermal magnetizations at 2 K for compounds **2** and **3**. Solid lines are the best fits to the Brillouin function for $S = 1/2$ (see text).

Heisenberg $S = 1/2$ chains. A very satisfactory agreement with the experimental data in the whole temperature range was obtained with $J = -0.07(2) \text{ cm}^{-1}$ and $g = 2.12(1)$ (solid line in Figure 7). The low value of the exchange coupling is in agreement with the weak antiferromagnetic interactions expected for similar Cu chains linked through –NC–C–CN– bridges.^{5,6}

For compound **3**, the thermal variation of the product of the molar magnetic susceptibility times the temperature ($\chi_m T$) shows a constant value of about $0.42 \text{ emu K mol}^{-1}$ from room temperature down to about 50 K (Figure 7). Below this temperature the $\chi_m T$ product shows a weak decrease, indicative of the presence of weak antiferromagnetic interactions, reaching a value of $0.37 \text{ emu K mol}^{-1}$ at 2 K (Figure 7). According to the chain structure observed for compound **3**, we have also fitted the susceptibility data using the empirical expression proposed by Hatfield^{18,19} for antiferromagnetic 1D isotropic Heisenberg $S = 1/2$ chains. A satisfactory agreement with the experimental data in the whole temperature range was obtained with $J = -0.18(1) \text{ cm}^{-1}$ and $g = 2.13(1)$ (solid line in Figure 7).

The paramagnetic behavior of compounds **2** and **3** is confirmed by the isothermal magnetizations of these compounds at 2 K that can be very well reproduced with a Brillouin function for an $S = 1/2$ with slightly reduced g factors that accounts for the weak antiferromagnetic interactions that can be observed at low temperatures (Figure 8).

Conclusions

This study reports three new examples of the copper(II)–tcpd system in which two different neutral ligands are introduced as co-ligands. Compound **1** which involves a bridging polynitrile and a bis-chelating bpym is described as mono-dimensional chain. The use of a chelating ligand (tn) instead of the bridging bpym led us to compound **2** with a 3D architecture and to compound **3** with a 1D structure. These structural differences clearly arise from the difference in the coordination modes of the tcpd²⁻ ligand (μ_2 -bridging mode in **1** and **3** and μ_4 -bridging mode in **2**). From the

(17) Bleaney, B.; Bowers, K. D. *Proc. R. Soc. (London) Ser. A* **1952**, *214*, 451.

(18) Kahn, O. *Molecular Magnetism*; VCH Publishers: New York, 1993.
(19) Brown, D. B.; Donner, J. A.; Hall, J. W.; Wilson, S. R.; Wilson, R. B.; Hodgson, D. J.; Hatfield, W. E. *Inorg. Chem.* **1979**, *18*, 2635.

magnetic point of view, this study shows that in **1** the magnetic interactions are dominated by the superexchange pathway through the bis-chelating bpym ligand, while in **2** and **3** the polynitrile ligand allows weak but significant antiferromagnetic interactions between paramagnetic centers. Thus, extension of this study to the paramagnetic polynitrile radical anions such as $[\text{C}_{10}\text{N}_8]^{•-20}$ and to other magnetic metal ions should lead to new magnetic systems with stronger magnetic exchange couplings.

(20) Decoster, M.; Conan, F.; Kubicki, M.; Le Mest, Y.; Richard, P.; Sala Pala, J.; Toupet, L. *J. Chem. Soc., Perkin Trans. 2* **1997**, 265.

Acknowledgment. The authors gratefully acknowledge the CNRS (Centre National de la Recherche Scientifique) and the framework of a French-Spanish Integrated Action (PICASSO 2004/N° 07137XK and HF2003-258) for financial support. F.T. thanks the Ministère de l'Éducation Nationale, de la Recherche et de la Technologie for a thesis grant.

Supporting Information Available: X-ray crystallographic files in CIF format. This material is available free of charge via the Internet at <http://pubs.asc.org>.

IC050235H